

Non-Holonomic Control IV : Coherence  
Protection in a Rubidium isotope

E. Brion

*Laboratoire Aimé Cotton,  
CNRS II, Bâtiment 505,  
91405 Orsay Cedex, France.*

V.M. Akulin

*Laboratoire Aimé Cotton,  
CNRS II, Bâtiment 505,  
91405 Orsay Cedex, France.*

D. Comparat

*Laboratoire Aimé Cotton,  
CNRS II, Bâtiment 505,  
91405 Orsay Cedex, France.*

I. Dumer

*College of Engineering,  
University of California,  
Riverside, CA 92521, USA.*

V. Gershkovich

*Institut des Hautes Etudes Scientifiques,  
Bures-sur-Yvette, France.*

G. Harel

*Department of Computing,  
University of Bradford,  
Bradford, West Yorkshire BD7 1DP, United Kingdom.*

G. Kurizki

*Department of Chemical Physics,  
Weizmann Institute of Science,  
76100 Rehovot, Israel.*

I. Mazets

*Department of Chemical Physics,  
Weizmann Institute of Science,  
76100 Rehovot, Israel.  
A.F. Ioffe Physico-Technical Institute,  
194021 St. Petersburg, Russia.*

P. Pillet

*Laboratoire Aimé Cotton,  
CNRS II, Bâtiment 505,  
91405 Orsay Cedex, France.*

December 24, 2018

### Abstract

In this paper, we present a realistic application of the coherence protection method proposed in the previous article. A qubit of information encoded on the two spin states of a Rubidium isotope is protected from the action of electric and magnetic fields.

## 1 Introduction

The coherence protection method presented in the previous article is applied to a Rubidium isotope, in which the information part corresponds to the spin of the exterior electron, whereas the orbital part of the wavefunction plays the role of the ancilla.

The different steps of our protection method are illustrated on this specific example. Adding the ancilla is achieved through pumping the atom from the level 5s into the shell 60f. The coding and decoding matrices are applied through the non-holonomic control technique. Finally, the protection step is achieved through the simultaneous emissions of three photons : two emissions are stimulated, whereas the third is spontaneous and constitutes the irreversible process needed in this step.

The paper is organized as follows. In the second section, we present the system and motivate our choice. In the third section we review each step of our method in detail and show their implementations on this specific physical configuration. Moreover, experimental problems and limitations are discussed.

## 2 Presentation of the system

In this paper, we show how to protect one qubit of information encoded on the two spin states of the ground level 5s of the radioactive isotope  $^{78}\text{Rb}$  against the action of  $M = 6$  error-inducing Hamiltonians  $\hat{E}_m$ . For numerical calculations we considered 3 magnetic Hamiltonians

$$\left\{ \hat{E}_k^\beta \propto \hat{L}_k + 2\hat{S}_k, k = x, y, z \right\},$$

and 3 electric Hamiltonians of second order

$$\left\{ \hat{E}_{k,l}^\varepsilon \propto \hat{r}_k^2 - \hat{r}_l^2, k, l = x, y, z, k < l \right\}.$$

Let us first motivate the choice of the Rubidium atom. Alkali atoms like Rb are very interesting for our purpose because of their hydrogen-like behavior : indeed, such an atom is the "natural" compound of an information subsystem, the spin part of the wavefunction, and an ancilla, the orbital part of the quantum state. As we shall see, one can easily increase the dimensionality of the ancilla by

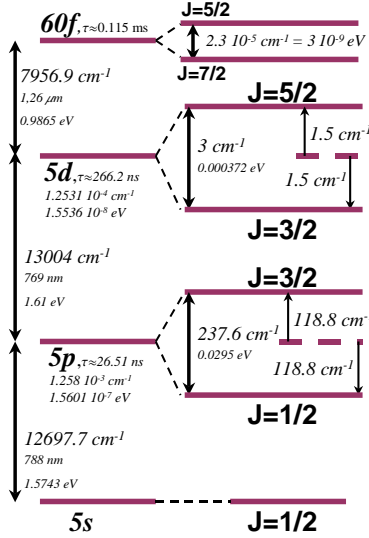


Figure 1: Spectrum of  $^{78}\text{Rb}$ : The useful part of the spectrum of Rubidium is represented.

simply pumping the atom towards a shell of higher orbital angular momentum  $L$ .

Among all alkali systems we chose  $^{78}\text{Rb}$  because of its spectroscopic features (Fig.1): in particular,  $^{78}\text{Rb}$  has no hyperfine structure (its nuclear spin is 0) which ensures that the ground level  $5s$  is degenerate (this is necessary for the projection scheme as we shall see below). Moreover it has a long enough lifetime ( $\tau \simeq 17.66 \text{ min}$ ) for the proposed experiment.

### 3 The different steps of the method

We shall now review each step of our method in detail. The information we want to protect is initially encoded on the two spin states  $|\nu_1\rangle = |5s, j = \frac{1}{2}, m_j = -\frac{1}{2}\rangle$  and  $|\nu_2\rangle = |5s, j = \frac{1}{2}, m_j = \frac{1}{2}\rangle$  of the ground level  $5s$  of the atom: the two-dimensional ( $I = 2$ ) information space  $\mathcal{H}_I = \text{Span}[|\nu_1\rangle, |\nu_2\rangle]$  is spanned by these two states. The first step of our scheme consists in adding an ancilla  $\mathcal{A}$  to the information system. In the present setting, the role of  $\mathcal{A}$  is played by the orbital part of the wavefunction. In the ground state ( $L = 0$ ), its dimension is  $A = 2L + 1 = 1$  (roughly speaking, there is no ancilla). If we want to protect one qubit of information against  $M = 6$  error-inducing Hamiltonians, we have to increase the dimensionality of the ancilla up to  $A = M + 1 = 7$  (according to the Hamming bound presented in the previous paper), by pumping the atom towards a shell  $nf$  ( $L = 3$ ). We choose the highly excited Rydberg state  $60f$

so as to make the fine structure as weak as possible (the splitting for  $60f$  is approximately  $10^{-5}cm^{-1}$ ), which shall be neglected in a first approach : thus, the  $N = I \times A = 2 \times 7 = 14$  basis vectors of the total Hilbert space  $\mathcal{H} = \mathcal{H}_I \otimes \mathcal{H}_A$  are almost perfectly degenerate ; the validity of this approximation will be discussed at the end of this section. To be more specific, the pumping is done in the following way

$$\begin{aligned} |\nu_1\rangle &\longrightarrow |\gamma_1\rangle = \left| 60f, j = \frac{5}{2}, m_j = -\frac{3}{2} \right\rangle \\ |\nu_2\rangle &\longrightarrow |\gamma_2\rangle = \left| 60f, j = \frac{5}{2}, m_j = -\frac{1}{2} \right\rangle. \end{aligned}$$

In other words, using the terminology of the previous sections, the information initially stored in  $\mathcal{H}_I$  is transferred into

$$\mathcal{C} = Span \left[ |\gamma_1\rangle = \left| 60f, j = \frac{5}{2}, m_j = -\frac{3}{2} \right\rangle, |\gamma_2\rangle = \left| 60f, j = \frac{5}{2}, m_j = -\frac{1}{2} \right\rangle \right].$$

The choice of the subspace  $\mathcal{C}$  might appear arbitrary at this stage, but it will be justified later by the practical feasibility of the projection process onto  $\mathcal{C}$ . Note that  $\mathcal{C}$  is an "entangled" subspace, whose basis vectors  $\{|\gamma_i\rangle\}_{i=1,2}$  are generic entangled states of the spin and orbital parts: this means that the projection step will not consist in a simple measurement of the ancilla but will involve a more intricate process we shall describe in detail later.

Practically, the pumping can be achieved as follows. Three lasers are applied to the atom: the first laser is right polarized and slightly detuned from the transition ( $5s \leftrightarrow 5p$ ) whereas the second and third lasers are left polarized and slightly detuned from the transitions ( $5p_{\frac{3}{2}} \leftrightarrow 5d_{\frac{3}{2}}$ ) and ( $5d_{\frac{3}{2}} \leftrightarrow 60f$ ) respectively. The role of the detunings is to forbid real one-photon processes: thus, the atom can only absorb three photons simultaneously and is thereby excited from the ground level  $5s$  to the Rydberg level  $60f$ . By using selection rules, one can construct the allowed paths represented on Fig.2: these paths only couple  $|\nu_1\rangle$  and  $|\nu_2\rangle$  to  $|\gamma_1\rangle$  and  $|\gamma_2\rangle$ , respectively.

The second step consists in imposing the coding matrix to the system by the non-holonomic control technique: to this end, we submit the atom to  $n_C = 34$  control pulses of timings  $\{t_i\}_{i=1,\dots,34}$ , during which two different combinations of magnetic and Raman electric Hamiltonians are alternately applied (see Fig.3). To be more explicit, during odd-numbered pulses ("A" type pulses) we apply the constant magnetic field

$$\vec{B} = \begin{pmatrix} B_x = 7 \cdot 10^{-3} T \\ B_y = 8.2 \cdot 10^{-3} T \\ B_z = -6.8 \cdot 10^{-3} T \end{pmatrix}$$

associated with the Zeeman Hamiltonian  $\widehat{W}_Z$ , and two sinusoidal electric laser

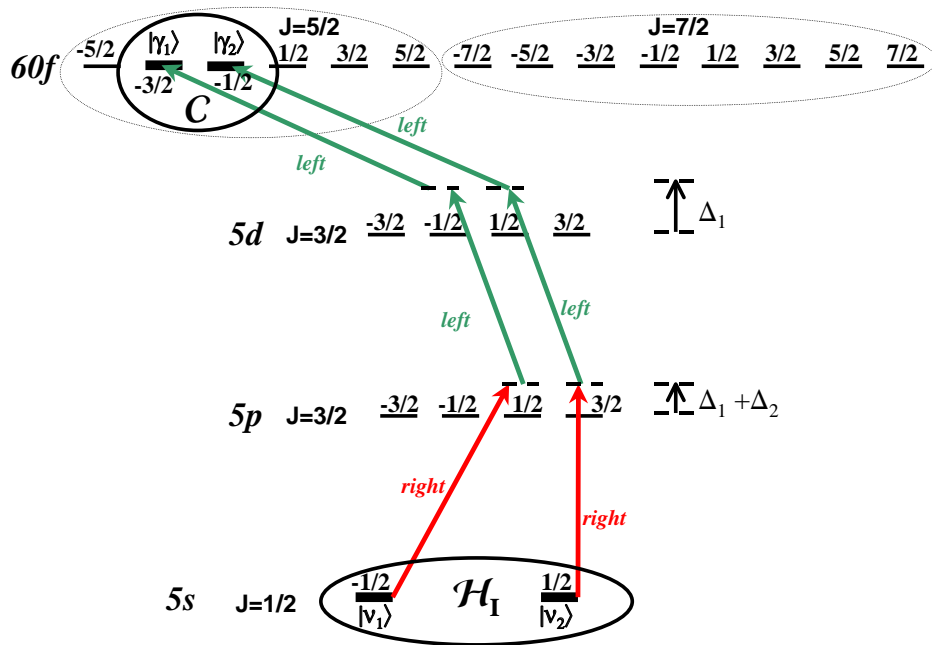


Figure 2: Ancilla adding by Pumping. Photon polarization and involved sub-Zeeman levels are represented.

fields

$$\vec{E}_a(t) = \text{Re} \left[ \vec{E}_a e^{-i\omega_R t} \right], \vec{E}'_a(t) = \text{Re} \left[ \vec{E}'_a e^{-i\omega'_R t} \right],$$

$$\vec{E}_a = \begin{vmatrix} E_{x,a} \\ E_{y,a} e^{-i\varphi_{y,a}} \\ 0 \end{vmatrix}, \vec{E}'_a = \begin{vmatrix} E'_{x,a} \\ E'_{y,a} e^{-i\varphi'_{y,a}} \\ 0 \end{vmatrix},$$

whose frequencies  $\omega_R$  and  $\omega'_R$  are respectively slightly detuned from the two transitions ( $60f \leftrightarrow 5d, j = \frac{3}{2}$ ) and ( $60f \leftrightarrow 5d, j = \frac{5}{2}$ ) (detunings  $\delta$  and  $\delta'$ ). The characteristic values of these fields are

$$\begin{aligned} E_{x,a} &= E'_{x,a} = 8.5 \cdot 10^5 \text{V.m}^{-1} \\ E_{y,a} &= E'_{y,a} = 5.2 \cdot 10^6 \text{V.m}^{-1} \\ \varphi_{y,a} &= \varphi'_{y,a} = 2.3 \\ \hbar\omega_R &= 0.986324 \text{ eV} = 7955.14 \text{ cm}^{-1} \\ \delta &= -0.000010 \text{ eV} = -0.080654 \text{ cm}^{-1} \\ \hbar\omega'_R &= 0.986676 \text{ eV} = 7958.14 \text{ cm}^{-1} \\ \delta' &= 0.000010 \text{ eV} = 0.080654 \text{ cm}^{-1}. \end{aligned}$$

The intensity of the laser beams are typically of the order of  $2 \cdot 10^8 \text{W.cm}^{-1}$ . The Raman Hamiltonian associated with these fields is denoted by  $\widehat{W}_{R,A}$  and the total perturbation is  $\widehat{P}_a = \widehat{W}_Z + \widehat{W}_{R,A}$ . During even-numbered pulses ("B" type pulses), we apply the same magnetic field as for A type pulses, which is experimentally convenient, and two sinusoidal electric laser fields

$$\vec{E}_b(t) = \text{Re} \left[ \vec{E}_b e^{-i\omega_R t} \right], \vec{E}'_b(t) = \text{Re} \left[ \vec{E}'_b e^{-i\omega'_R t} \right],$$

$$\text{where } \vec{E}_b = \begin{vmatrix} E_{x,b} \\ E_{y,b} e^{-i\varphi_{y,b}} \\ 0 \end{vmatrix}, \vec{E}'_b = \begin{vmatrix} E'_{x,b} \\ E'_{y,b} e^{-i\varphi'_{y,b}} \\ 0 \end{vmatrix},$$

whose frequencies are the same as above and whose characteristic values are

$$\begin{aligned} E_{x,b} &= E'_{x,b} = -5.2 \cdot 10^6 \text{V.m}^{-1} \\ E_{y,b} &= E'_{y,b} = 8.5 \cdot 10^5 \text{V.m}^{-1} \\ \varphi_{y,a} &= \varphi'_{y,a} = 2.3. \end{aligned}$$

The Raman Hamiltonian associated with these fields is denoted by  $\widehat{W}_{R,B}$ . The corresponding perturbation is  $\widehat{P}_b = \widehat{W}_Z + \widehat{W}_{R,B}$ . As the fine structure of the level  $60f$  is neglected, the unperturbed Hamiltonian  $\widehat{H}_0$  is 0 and the total Hamiltonian has the following form:  $\widehat{H}_a = \widehat{P}_a$  during "A" pulses,  $\widehat{H}_b = \widehat{P}_b$  during "B" pulses. The 34 different timings have been calculated so that

$$\widehat{U}(\tau_1, \dots, \tau_{34}) = e^{-i\widehat{H}_B \tau_{34}} e^{-i\widehat{H}_A \tau_{33}} \dots e^{-i\widehat{H}_A \tau_1} = \widehat{C}$$

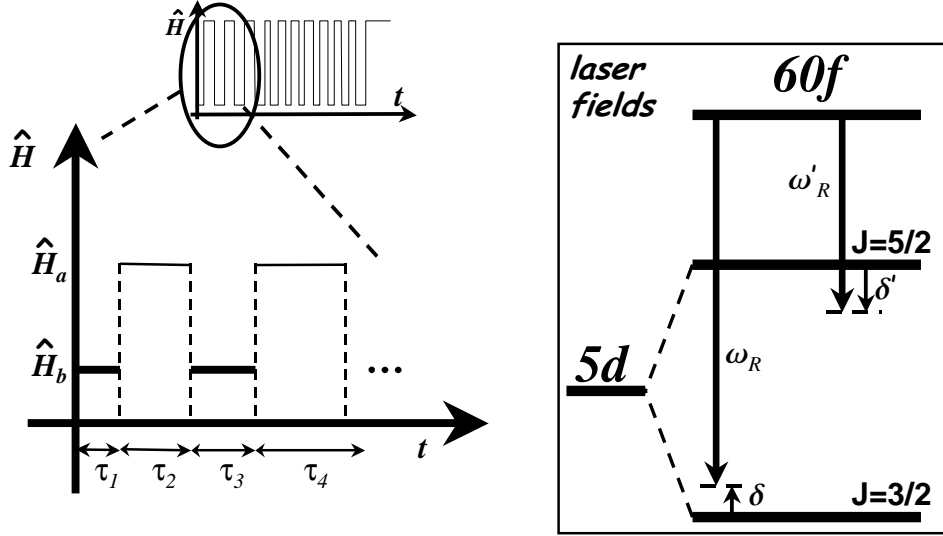


Figure 3: Coding step through the non-holonomic control technique. The two Hamiltonians  $\hat{H}_a$  and  $\hat{H}_b$  are alternately applied to the system during pulses of timings  $\{\tau_i(ns)\} = \{3.9763, 6.4748, 4.2274, 3.6259, 2.8717, 3.6281, 7.2263, 6.4260, 4.8070, 5.0394, 6.5242, 4.8890, 4.2400, 7.3834, 4.8653, 5.4799, 4.5341, 4.3099, 6.2959, 3.7346, 6.5293, 6.8586, 6.0749, 5.1213, 4.6806, 3.4985, 3.9909, 4.6701, 4.5168, 6.4702, 4.7787, 5.3476, 3.4567, 3.8009\}$ . The frequencies of the laser fields involved in the encoding step are represented on the spectrum of the Rubidium atom. The fine structure of the Rydberg level  $60f$  is not represented.

checks the correction conditions presented in the previous paper. At the end of the coding step, the information is transferred into the code space  $\tilde{\mathcal{C}} = \tilde{\mathcal{C}}\mathcal{C}$ , encoded on the codewords  $\{|\tilde{\gamma}_i\rangle = \tilde{\mathcal{C}}|\gamma_i\rangle\}_{i=1,2}$ .

As one can see on Fig.3, the total duration of a control period ( $\simeq 125ns$ ) is approximately  $10^3$  times shorter than the lifetime of  $60f$  Rydberg state which is approximately  $0.115ms$ , and the different pulse timings range between  $2.9ns$  and  $7.4ns$ , which are feasible.

After a short time, due to the action of the error Hamiltonians, the information stored in the system acquires a small erroneous component, which is orthogonal to the code space  $\tilde{\mathcal{C}}$ . Then, we decode the information through the application of the matrix  $\hat{\mathcal{C}}^{-1}$ . To this end, we reverse  $\vec{B}$  and the detunings  $\delta$  and  $\delta'$ , while leaving all the other values unchanged (this amounts to taking the opposite of Hamiltonians  $\hat{H}_a$  and  $\hat{H}_b$ ), and apply the same sequence of control pulses backwards: we start with an "A" pulse whose timing is  $\tau_{34}$ , then apply a "B" pulse during  $\tau_{33}$ , etc. (see Fig.4). The decoding step yields an erroneous

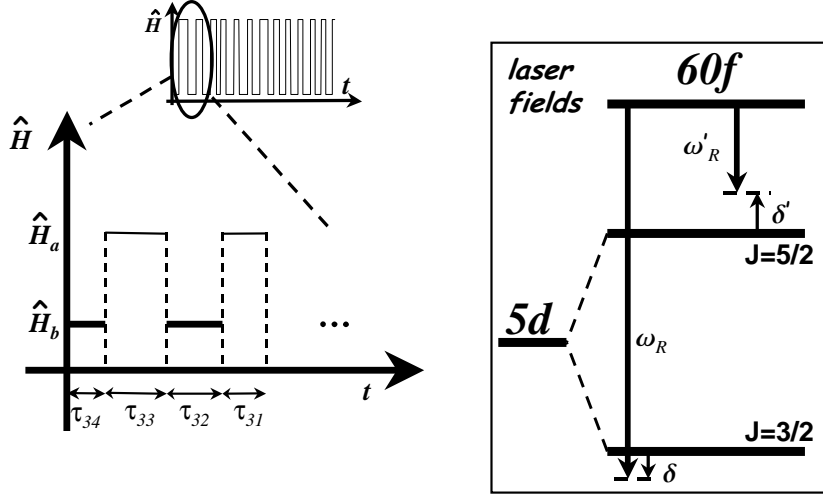


Figure 4: Decoding step through the non-holonomic control technique. We reverse the magnetic field and the detunings of electric fields, as represented on the spectrum of the Rubidium atom, and apply the same control sequence as for coding (same timings) in the reverse way.

state whose projection onto  $\mathcal{C}$  is the initial information state.

In the last step, we project the erroneous state vector onto the subspace  $\mathcal{C}$  to recover the initial information. Projection is a non-unitary process which cannot be achieved through a Hamiltonian process, but requires the introduction of irreversibility. To this end, we make use of a path which is symmetric with the pumping step, consisting in two stimulated and one spontaneous emissions. To be more explicit, we apply two left circularly polarized lasers (see Fig.5) slightly detuned from the transitions ( $60f \leftrightarrow 5d, j = \frac{3}{2}$ ) and ( $5d, j = \frac{3}{2} \leftrightarrow 5p, j = \frac{3}{2}$ ). Due to these laser fields, the atom is likely to fall towards the ground state and emit two stimulated and one spontaneous photons.

If a circularly right-polarized spontaneous photon is emitted, the selection rules show that the only states to be coupled to the ground level are  $|\gamma_1\rangle$  and  $|\gamma_2\rangle$  to  $|\nu_1\rangle$  and  $|\nu_2\rangle$ , respectively (see Fig.5). In other terms, the emission of such a spontaneous photon brings the "correct" part of the state vector back into  $\mathcal{H}_I = \text{Span} [|\nu_1\rangle, |\nu_2\rangle]$ . On the contrary, the other cases - "left-polarized", "linearly-polarized spontaneous photon", or "no photon at all" - do not lead to the right projection process.

The "left-polarized photon" and "no photon emitted" cases are quite unlikely, since their probability is proportional to the square of the error amplitude, that is to the square of the very short Zeno interval. By contrast, the "linearly polarized photon" case is quite annoying because it mixes the two paths  $|\gamma_1\rangle \rightarrow |\nu_1\rangle$  and  $|\gamma_2\rangle \rightarrow |\nu_2\rangle$ : one has to get rid of this parasitic pro-



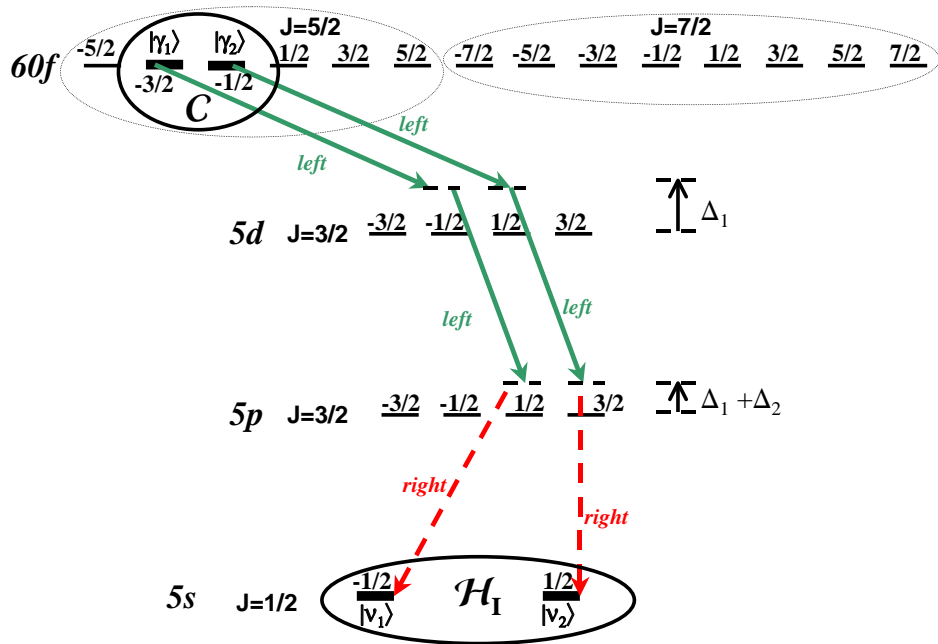


Figure 5: Projection path. The lasers involved are marked by solid arrows, the spontaneous photon is represented by a dashed arrow. The different polarizations are specified. The fine structure of the level  $60f$  is not represented.

cess by minimizing its relative probability with respect to the process followed by the "right-polarized" photon emission. This can be achieved by launching the  $^{78}\text{Rb}$  atom, previously cooled, into a Fabry-Perot cavity, in an atomic fountain manner (fine tuning of the lasers driving the  $60f-5d$  and  $5d-5p$  transition will be necessary to avoid reflection of the external laser radiation from the cavity). The decay rate for the 3-photon transition  $|\gamma_i\rangle \rightarrow |\nu_i\rangle$  is

$$\Gamma_{\gamma_i\nu_i} = 2\pi \left| \frac{d_{\gamma_i\lambda_j} E_1}{\hbar\Delta_1} \right|^2 \left| \frac{d_{\lambda_j\mu_k} E_2}{\hbar(\Delta_1 + \Delta_2)} \right|^2 \overline{2\pi\hbar ck_s \left| \vec{d}_{\mu_k\nu_i} \vec{e}_R^* \right|^2 \varrho(\vec{k}_s)},$$

where  $\vec{k}_s$  denotes the wave vector of the spontaneously emitted photon,  $\vec{e}_R$  is the left-polarized photon polarization unit vector,  $\varrho(\vec{k}_s)$  is the density of states (normalized to the cavity volume) for the cavity field at  $\vec{k}_s$ , and the bar denotes averaging over the directions of  $\vec{k}_s$ . The transition dipole moments are denoted by  $d_{ab}$ : during the projective process the states coupled to  $|\gamma_1\rangle$  and  $|\gamma_2\rangle$  are

$$\left\{ |\lambda_1\rangle = \left| 5d, j = \frac{3}{2}, m_j = -\frac{1}{2} \right\rangle, |\lambda_2\rangle = \left| 5p, j = \frac{3}{2}, m_j = +\frac{1}{2} \right\rangle \right\},$$

$$\left\{ |\mu_1\rangle = \left| 5d, j = \frac{3}{2}, m_j = \frac{1}{2} \right\rangle, |\mu_2\rangle = \left| 5p, j = \frac{3}{2}, m_j = \frac{3}{2} \right\rangle \right\}.$$

respectively.

The presence of the cavity enhances the density of states for the modes propagating paraxially to the  $z$ -axis and ensures that

$$\Gamma_{\gamma_1\nu_1}, \Gamma_{\gamma_2\nu_2} \gg \left| \frac{d_{\gamma_i\lambda_j} E_1}{\hbar\Delta_1} \right|^2 \left| \frac{d_{\lambda_j\mu_k} E_2}{\hbar(\Delta_1 + \Delta_2)} \right|^2 \gamma,$$

where  $\gamma$  is the decay rate of  $\left| 5p, j = \frac{3}{2}, m_j = +\frac{1}{2} \right\rangle$  into  $\left| 5s, j = \frac{1}{2}, m_j = +\frac{1}{2} \right\rangle$ , so that the undesired process followed by the  $\pi$ -photon emission is relatively less important than it were in free space. The dynamics of the density matrix elements  $\rho_{ab}$  is governed by the following system ( $i = 0, 1$ ):

$$\begin{aligned} \dot{\rho}_{\gamma_i\gamma_i} &= -\Gamma_{\gamma_i\nu_i} \rho_{\gamma_i\gamma_i}, \\ \dot{\rho}_{\nu_i\nu_i} &= \Gamma_{\gamma_i\nu_i} \rho_{\gamma_i\gamma_i}, \\ \dot{\rho}_{\gamma_1\gamma_2} &= -\frac{1}{2}(\Gamma_{\gamma_1\nu_1} + \Gamma_{\gamma_2\nu_2}) \rho_{\gamma_1\gamma_2}, \\ \dot{\rho}_{\nu_1\nu_2} &= \sqrt{\Gamma_{\gamma_1\nu_1} \Gamma_{\gamma_2\nu_2}} \rho_{\gamma_1\gamma_2}. \end{aligned}$$

To avoid dephasing which would corrupt the information, the coherence matrix element  $\rho_{\gamma_1\gamma_2}$  must be transferred with the maximum efficiency  $\eta$

$$\eta = \frac{2\sqrt{\Gamma_{\gamma_1\nu_1} \Gamma_{\gamma_2\nu_2}}}{\Gamma_{\gamma_1\nu_1} + \Gamma_{\gamma_2\nu_2}}$$

into  $\rho_{\nu_1\nu_2}$ . According to the Wigner-Eckart theorem, we have

$$\frac{\Gamma_{\gamma_1\nu_1}}{\Gamma_{\gamma_2\nu_2}} = \left( \frac{C_{3/2 \ -1/2 \ 1 \ -1}^{5/2 \ -3/2} C_{3/2 \ 1/2 \ 1 \ -1}^{3/2 \ -1/2} C_{1/2 \ -1/2 \ 1 \ 1}^{3/2 \ 1/2}}{C_{3/2 \ 1/2 \ 1 \ -1}^{5/2 \ -1/2} C_{3/2 \ 3/2 \ 1 \ -1}^{3/2 \ 1/2} C_{1/2 \ 1/2 \ 1 \ 1}^{3/2 \ 3/2}} \right)^2,$$

whence  $\eta = 12\sqrt{2}/17 \approx 0.99827$ . In other words, the probability of error during the Zeno projection stage due to the small difference of the Clebsch-Gordan coefficient products for the two paths is equal to or less than  $1 - \eta \approx 0.00173$  (the equality is reached if the initial state is  $(|0\rangle \pm |1\rangle)/\sqrt{2}$ ). Note that the states  $60f$ ,  $5d$ , and  $5p$  have finite lifetimes  $\tau_k$  (see Fig.1). Thus the transition rates  $\Gamma_{\gamma_i\nu_i}$  must be much larger than  $1/\tau_{60f}$ ,  $\left| \frac{d_{\gamma_i\lambda_j} E_1}{\hbar\Delta_1} \right|^2 / \tau_{5d}$ , and  $\left| \frac{d_{\gamma_i\lambda_j} E_1}{\hbar\Delta_1} \right|^2 \left| \frac{d_{\lambda_j\mu_k} E_2}{\hbar(\Delta_1 + \Delta_2)} \right|^2 / \tau_{5p}$ , in order to minimize errors caused by the decay of these unstable states.

To complete the projection step, one has now to transfer the atom back into its coherent superposition on the shell  $60f$ : this is achieved by the same pumping sequence as in the first step. The mismatch of the Clebsch-Gordan coefficient products will cause again the error probability  $1 - \eta$ . The information is then restored with very high probability and the system is ready to undergo a new protection cycle.

Until now, we have neglected the fine structure splitting of the level  $60f$ , which is approximately  $2.10^{-5} cm^{-1}$  and corresponds to a period  $\tau_f \sim 1.5\mu s$ . To conclude this section, we shall now take it into account and see how it affects each step of our scheme.

Obviously the pumping and projection steps will not be affected by the fine structure, since the information-carrying vectors  $\{|\gamma_1\rangle, |\gamma_2\rangle\}$  belong to the same multiplet ( $J = 5/2$ ).

The coding and decoding steps are neither modified by the existence of the fine structure. Since the typical period of the fine structure Hamiltonian  $\tau_f \sim 1.5\mu s$  is more than 10 times longer than the total duration of the coding or decoding steps, it is legitimate to neglect its effect.

The influence of the fine structure on the free evolution period during which errors are likely to occur is more complicated to study in the general case. However, two simple limiting regimes can be considered. If the spectrum of the coupling functions  $f_m(t)$ 's is very narrow (*i.e.* if the variation timescale of the  $f_m(t)$ 's is much longer than  $\tau_f$ ), one can show that our scheme applies directly as though there were no fine structure, provided the error Hamiltonians  $\{\widehat{E}_m\}$  are replaced by  $\{\widehat{E}_m^{(0)}\}$ , where  $\widehat{E}_m^{(0)}$  is obtained from  $\widehat{E}_m$  by simply setting to zero the rectangular submatrices which couple the two multiplets ( $J = 5/2, 7/2$ ). The second limiting regime corresponds to a very broad spectrum for the  $f_m(t)$ 's (variation timescale much shorter than  $\tau_f$ ): in that case, one can show that our scheme applies provided one chooses a Zeno interval multiple of  $\tau_f$ .

Finally, it must be emphasized that Rydberg atoms, though long-lived are also very sensitive to collisional processes as well as Doppler effects, which result in a fast coherence loss ; nevertheless, we hope that in a single (or few) atom experiment using cold atoms the coherence lifetime can be extended to hundreds of  $ns$ . These effects have been omitted in all this section in which we just intended to provide a pedagogical demonstration of our method on a simple physical system ; but an experimentally feasible setup should obviously deal with these unavoidable drawbacks of Rydberg states.

## 4 Conclusion

In this paper, a realistic application of our coherence protection method has been proposed : it has been shown that, in principle, one qubit of information encoded on the spin states of a Rubidium isotope can be protected from the action of parasitic electric and magnetic fields. The different steps of our technique can be implemented on this specific example : adding the ancilla is achieved through pumping ; information is coded and decoded through non-holonomic control ; projection is achieved by a three-photon process, involving spontaneous emission.

Practical feasibility of our scheme has been discussed, and experimental problems have been raised. However relevant, these limitations do not restrict the applicability of our method, and the pedagogical example considered here demonstrates its implementability.